Adsorptive properties of metal oxide dispersed carbon materials and characterization of metal oxide fine particles by XAFS

Yoshiyuki Hattori[a]* and Katsumi Kaneko[b]

[a]Center for Frontier Electronics and Photonics, Chiba University, 1-33 Yayoi, Inage, Japan, and [b]Graduate School for Science, Chiba University, 1-33 Yayoi-cho, Inage, Chiba 263-8522. E-mail: hattori@pchem2.s.chiba-u.ac.jp

Surface modification of activated carbon fiber (ACF) with metal oxide increases the adsorptivity of the ACF for supercritical gas such as NO and CH_4. In this study, pitch-based activated carbon fibers (P20) were modified with nickel oxide particles. The adsorptive properties and micropore structures of NiO dispersed P20 (NiO-P20) were investigated by nitrogen adsorption isotherms at 77 K. The isotherm was of type I, suggesting that the NiO-P20 has microporosity. The micropore volume and surface area for NiO-dispersed P20 were smaller than that of P20 by about 15%. The Ni *K*-edge X-ray absorption fine structure of NiO-P20 has been investigated in order to characterize the species dispersed on P20. The local structure of the NiO particles on the P20 showed some different features compared with the local structure of powdered NiO.

Keywords: activated carbon fibers; **nickel oxide**; **adsorptive properties.**

1. Introduction

Activated carbon fibers (ACFs) are representative porous carbon materials and have potentials for wide practical applications. ACFs have been used in the various technologies, because of their characteristic adsorption properties. It is well known that their adsorption properties are mainly caused by the uniform micropores. The adsorption of vapors in micropores is enhanced by overlap of the potential fields from opposite pore-walls (Dubinin, 1960, Everett & Powl, 1976, Gregg & Sing, 1982). The phenomenon is called micropore filling (Marsh, 1987, Carrott *et al.*, 1987, McEnaney, 1987), which is an enhanced physical adsorption and usually a dominant process for a vapor. Therefore, the microporous solid has great adsorption capacity and adsorption rate for vapors by micropore filling. Nevertheless, micropore filling is a predominant process only for vapor and is not effective for the supercritical gas due to small molecular interactions. The development of good adsorbent for a supercritical gas is very important in the field of the study on the energy storage materials and removal of atmospheric pollutants. Recently, Kaneko *et al.* have prepared iron oxide-dispersed ACFs which adsorb large amount of supercritical NO at 303 K by chemisorption-assisted micropore filling (Kaneko *et al.*, 1986, 1987, 1988, 1989). Ultra-fine iron oxides on the ACF assist the micropore filling of the supercritical NO. Also, Kaneko *et al.* have reported that the pitch-based ACFs modified with MgO and NiO fine particles give rise to a marked enhancement of methane adsorption (Kaneko *et al.*, 1993, 1997). These novel effects of fine metal oxide particles dispersed on ACFs are very interesting not only due to industrial applications but also to scientific aspects. It is important to characterize the dispersed metal oxide state in order to elucidate the role of metal oxides in chemisorption-assisted micropore filling. In this work, we characterize the porous structures of nickel oxide-dispersed ACFs and the local structures of dispersed nickel oxide particles by means of nitrogen adsorption isotherm at 77 K, X-ray adsorption near-edge structures (XANES), and extended X-ray adsorption fine structures (EXAFS).

2. Experimental

The pitch-based activated carbon fibers (P20) were evacuated at 383 K for 2 h in vacuo prior to the dispersion of NiO on P20. The pre-evacuated ACFs was immersed in the 30% $Ni(NO_3)_2$ solution at room temperature for 15, 40, or 90 h. Then, the solution with ACF was adjusted to pH 10 with 1 M NaOH solution. The P20 modified with $Ni(OH)_2$ was washed with distilled water and dried at 333 K. The $Ni(OH)_2$ dispersed P20 was heated at 573 K for 3 h in N_2 flow. Decomposition of the $Ni(OH)_2$ particles on P20 at 573 K gave NiO particles dispersed P20 (NiO-P20). The adsorption and desorption isotherms of pristine and modified P20 were measured by means of an automatic volmetric sorption analyzer (Aoutosorb-1) using nitrogen gas as adsorbate at 77 K. Samples were pre-evacuated at 383 K and 10^{-3} Pa prior to measurement N_2 adsorption. The XAFS measurements were carried out using a Technos EXAC820 with a rotating-anode X-ray source that was operated at 17 kV $\times$ 150 mA. The Ni *K*-edge XAFS spectra of NiO-P20, powdered NiO, and powdered $Ni(OH)_2$ were measured by using of the EXAC820 in transmission mode. Samples were adjusted in a sufficient quantity to give an edge jump of about 1. The program FEFF8 was used for the simulation of the EXAFS Fourier transform of NiO procedures (Ankudinov *et al.*, 1989). The theoretical phases and amplitudes obtained from FEFF8 were used for curve fitting.

3. Results and Discussion

Figure 1 shows the adsorption isotherms of N_2 at 77 K for pristine P20 and NiO dispersed P20 prepared by immersing into 30% $Ni(NO_3)_2$ solution for 15, 40, and 90 h. The isotherms are of type I isotherm, suggesting that NiO dispersed samples are microporous materials. The surface modification with NiO increases the amount of N_2 adsorption. The α_s-plot was applied to these N_2 adsorption isotherms using reference data of nonporous carbon black (Atkinson *et al.*, 1984, Sing, 1989, Kaneko *et al.*, 1992, 1998). The specific surface area a_s, external surface area a_{ext}, micropore volume v_m, and micropore width w are shown in Table 1. The NiO dispersion decreases both surface area and micropore volume. On the other hand, the micropore width is the same as that of pristine P20. These results suggest that the NiO dispersion partially blocks the micropores. Therefore, almost NiO particles should be dispersed in the micropores.

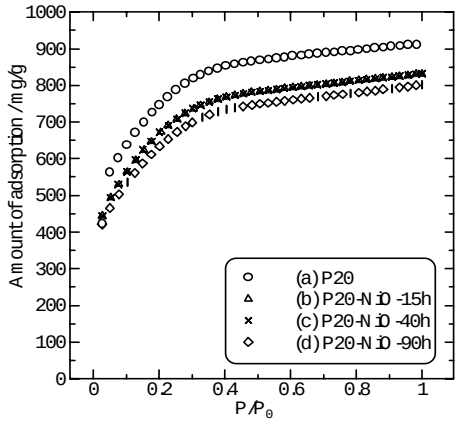

Figure 1
The N_2 adsorption isotherms of (a) P20 and NiO dispersed P20 prepared by immersing into 30(b) 15, (c) 40, and (d) 90 h.

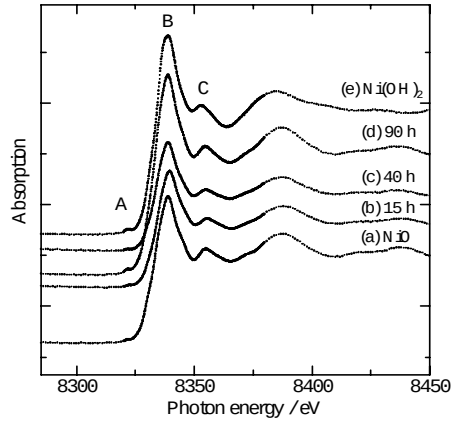

Figure 2
Ni *K*-edge XANES spectra of (a) NiO, (b) NiO-P20-15h, (c) NiO-P20-40h, (d) NiO-P20-90h, and (e) $Ni(OH)_2$.

Table 1
Micropore structural parameters of P20 and NiO dispersed P20.

sample name	a_s m^2/g	a_{ext} m^2/g	v_m ml/g	w nm
P20	1988	65	1.05	1.1
P20-NiO-15h	1780	141	0.873	1.1
P20-NiO-40h	1780	116	0.892	1.1
P20-NiO-90h	1680	100	0.866	1.1

X-ray absorption spectroscopic technique was applied to characterize NiO dispersed on P20. Figure 2 shows the XANES spectra of powdered NiO, NiO-P20, and powdered $Ni(OH)_2$. The spectra of all NiO-P20 are similar to that of powdered NiO. All spectra show a weak pre-edge peak, which arises from the 1*s*-3*d* forbidden transition in the case of the O_h symmetry around a Ni atom. The intensity of this peak is so weak that O_h symmetry is almost maintained irrespective of dispersion on P20. The peaks b and c are assigned to the 1*s*-4*p* transition and multiple scattering, respectively. The fact that the spectra of NiO-P20 are different from that of $Ni(OH)_2$, being close to that of NiO indicates the formation of NiO-like substances on P20.

Figure 3 shows the Ni *K*-edge EXAFS spectra of powdered NiO, NiO-P20, and powdered $Ni(OH)_2$. The edge-jump of the Ni *K*-edge is clearly observed and the EXFAS signal is well observed up to k = 12 $Å^{-1}$. Figure 4 shows the k^3 weighted Fourier transforms (without phase-shift correction) of $\chi(k)$ extracted the EXAFS spectra for powdered NiO, NiO-P20, and powdered $Ni(OH)_2$. There are 5 peaks (A-E) which are ascribed to Ni-O (A), Ni-Ni (B), Ni-O (C), Ni-Ni (D), and Ni-O (E) distances, respectively. All Fourier transforms for NiO-P20 have similar feature of that by NiO and are in agreement with that of simulation by FEFF8, suggesting the formation of NiO-like substance on the P20. However, the distance of peak A for sample (b) and (c) is somewhat larger than that of powdered NiO. In order to determine the accurate structural parameters, we used the *r* space method to curve fit the Fourier transform data. The results of best fits data for first and second shells are tabulated in Table 2. The Ni-O and Ni-Ni bond distances for NiO calculated from X-ray diffraction data are 2.09 and 2.95 Å, respectively. The bond distances for powdered NiO correspond to those calculated by x-ray diffraction data. On the other hand, the bond distances for NiO-P20 slightly larger than those of powdered NiO, and decrease with increase in the immersion time in $Ni(NO_3)_2$ solution. This indicates that the structural properties of the NiO particles on P20 are somewhat different from that of powdered NiO.

Table 2
First and second nearest-neighbor interatomic distances of powdered NiO and NiO dispersed P20. The error bars for all results are only less than 0.01 Å in distance. The values of bond distances for NiO* are from JCPDS card data.

	Ni-O (Å)	Ni-Ni (Å)
NiO	2.10	2.94
P20-NiO-15h	2.22	2.99
P20-NiO-40h	2.14	2.98
P20-NiO-90h	2.08	2.98
NiO*	2.09	2.95

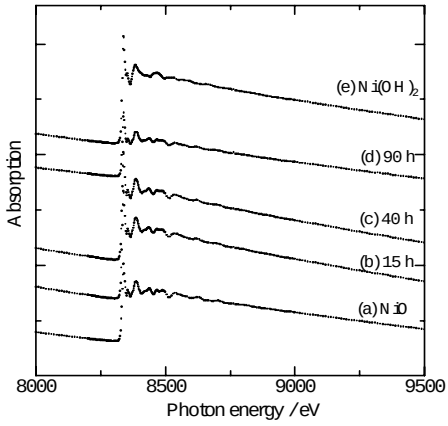

Figure 3
Ni *K*-edge EXAFS spectra of (a) NiO, (b) NiO-P20-15h, (c) NiO-P20-40h, (d) NiO-P20-90h, and (e) $Ni(OH)_2$.

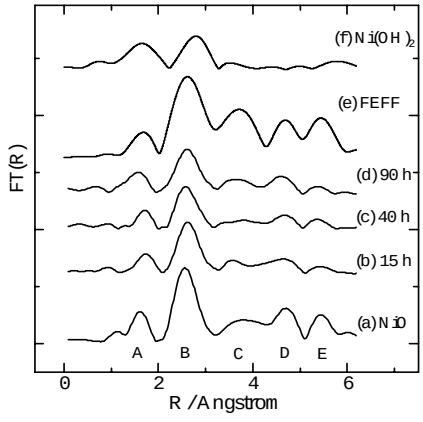

Figure 4
The k^3 weighted Fourier transforms of $\chi(k)$ extracted the EXAFS spectra for (a) NiO, (b) NiO-P20-15h, (c) NiO-P20-40h, (d) NiO-P20-90h, (e) simulation by FEFF8 with atomic position of NiO crystal, and (e) $Ni(OH)_2$.

4. Conclusions

The micropore structures of NiO dispersed activated carbon fibers (P20) were characterized by N_2 adsorption isotherm. All the adsorption isotherms for NiO-P20 are of type I isotherm, suggesting the presence of micropres. The adsorptive properties were improved by the surface modification with NiO. The Ni *K*-edge XANES and EXAFS spectra of NiO-P20 supported the formation of fine NiO particles in micropores of P20, although the local structure of NiO particles in the micropores is slightly different from that of powdered NiO.

Dr. Konishi and Mr. Kawai gave appropriate comments on the analysis of X-ray absorption spectra. This work was partially supported by the Proposal-Based New Industry Creative Type Technology R&D Promotion Program (99E10-0091) from NEDO.

References

Ankudinov, A. L., Ravel, B. & Rehr, J. J. (1998). *Phys. Rev.* **B58**, 7565–7579.

Atkinson, D. A., McLeod, A. L. & Sing, K. S. W. (1984). *J. Chem. Phys.* **81**, 791.

Carrott, P. J. M., Roberts, R. A. & Sing, K. S. W. (1987). *Carbon* **25**, 59–68.

Dubinin, M. M. (1960). *Chem. Rev.* **60**, 235.

Everett, D. H. & Powl, J. C. (1976). *J. Chem. Soc., Fraday Trams.* **25**, 619-636.

Gregg, S. J. & Sing, K. S. W. (1982). *Adsorption, Surface Area and Porosity*, p. 135. London: Academic Press.

Kaneko, K. (1987). *Langmuir* **3**, 26–32.

Kaneko, K., Ozeki, S. & Inouye, K. (1987). *Colloid & Polymer Sci.* **265**, 39–47.

Kaneko, K., Kobayashi, A., Suzuki, T., Ozeki, S., Kakei, K., Kosugi, N. & Kuroda, H. (1988). *J. Chem. Soc., Faraday Trans.* **84**, 1795–1805.

Kaneko, K. & Inouye, K. (1988). *Adsorption Sci. Tech.* **5**, 114–125.

Kaneko, K., Kosugi, N. & Kuroda, H. (1989). *J. Chem. Soc., Fraday Trans.* **85**, 869–881.

Matsumoto, A. & Kaneko, K. (1989). *J. Chem. Soc., Fraday Trans.* **85**, 3437–3450.

Kaneko, K & Shindo, N. (1989). *Carbon* **27**, 815–820.

Kaneko, K & Ishii, C. (1992). *Colloids Surf.* **67**, 203–212.

Kaneko, K., Murata, K., Shimizu, K., Camara, S. & Suzuki, T. (1993). *Langmuir* **9**, 1165–1167.

Kaneko, K & Murata, K. (1997). *Adsorption* **3**, 197–208.

Kaneko, K., Ishii, C., Kanoh, H., Hanzawa, Y., Setoyama, N. & Suzuki, T. (1998). *Adv. Colloid Interface Sci.* **76-77**, 295–320.

Marsh, H. (1987). *Carbon* **25**, 49–58.

McEnaney, B. (1987). *Carbon* **25**, 69–75.

Sing, K. S. W. (1989). *Carbon* **27**, 5-11.

Received 31 July 2000 • Accepted 8 November 2000